AiMT

Advances in Military Technology
Vol. 12, No. 2 (**2017**), pp. 301-310
ISSN 1802-2308, eISSN 2533-4123
DOI 10.3849/aimt.01201

Influence of Critical Flow in the Differentially Pumped Chamber AQUASEM

P. Hlavatá, J. Maxa*, M. Bílek, P. Vyroubal and R. Bayer

Department of Electrical and Electronic Technology, Faculty of Electrical Engineering and Communication, Brno University of Technology, Czech Republic

The manuscript was received on 7 June 2017 and was accepted after revision for publication on 8 December 2017.

Abstract:

The article deals with the effect of the critical flow, which is examined at pumping of the differential pumping chamber of the Environmental Scanning Electron Microscope (ESEM). The article compares the state of the flow in the area of pumped chamber at pressure ratio on the apertures when the critical flow occurs and its advantages in design of the chambers versus the flow without the clogging the nozzle. Problematics were solved using finite volume method by Ansys Fluent system.

Keywords:

Ansys Fluent, differentially pumped chamber, ESEM, SolidWorks

1. Introduction

Using the Environmental Scanning Electron Microscope (ESEM) is possible to observe samples, which contain water in their natural condition [1]. This can be achieved using a relatively high gas pressure in the specimen chamber, because examination of biological samples in low pressure is not possible due to their desiccation. Another advantage is that the sample does not need to be plated because it is not charged, thus the electron beam does not deflect. This allows us to observe samples containing greater or lesser quantity of water, liquid samples, and dielectric materials and after some adjustments it is even possible to observe chemically active samples, chemical reactions and biological processes.

Achieving and maintaining a higher pressure in the specimen chamber (as high as the pressure of 3 000 Pa) separated from the low pressure within the area of the electron source from 10^{-3} Pa to 10^{-9} Pa puts specific requirements on the design of the

* *Corresponding author: Department of Electrical and Electronic Technology, Faculty of Electrical Engineering and Communication, Brno University of Technology, Czech Republic. Phone: +420 54114 6129, fax: +420 54114 6129, E-mail: maxa@feec.vutbr.cz*

microscope and its pumping system. The microscope needs to be divided using apertures containing holes in the order of tens to hundreds of micrometers forming the differentially pumped chamber (PLA 1 and PLA 2 in Fig. 1) [2]. Using this way, we can achieve the lowest pressure possible on the optical axis of the microscope which is on the primary electron beam path, as well as we can maintain a high pressure in the specimen chamber at the same time. Usually a system of rotary, diffusion or turbo molecular vacuum pumps is used for the pumping of the interior of the specimen chamber and the adjacent differentially pumped chamber, or ion vacuum pumps for the source of electrons. In this case, it is still necessary to ensure the slowest desiccation of the sample possible.

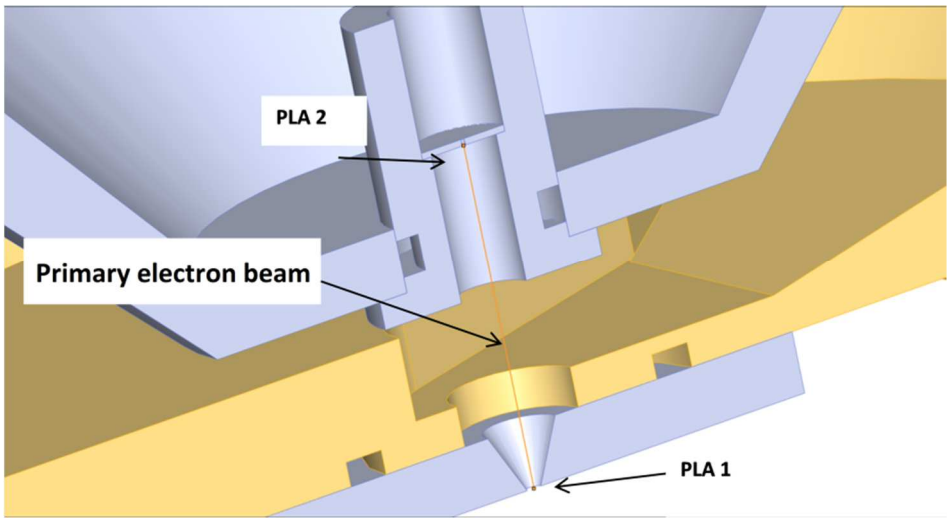

Fig. 1 Primary electron beam passing through a high-pressure environment in the differentially pumped chamber of AQUASEM II

Due to the higher gas pressure in the ESEM specimen chamber, there is an increased occurrence of interactions of electrons with molecules and atoms of gases (mainly water vapors) and subsequently the original primary electron beam diffuses [3]. The diffusion of primary electrons increases with increasing pressure, average atomic number of gas, working distance and decreasing accelerating voltage of the beam. This diffusion results in an increase in the diameter of the primary electron beam trajectory. In construction of ESEM, it is necessary to choose properly previous conditions. The non-acceptance of the previous conditions has such an effect that the signal/noise ratio in the detected signal is less favorable, and the final effect may deteriorate the resolution of the microscope [4].

2. AQUASEM

Environmental scanning electron microscope of AQUASEM type enables to observe soft tissue samples, dynamic events and reactions occurring in a gaseous or humid environment at higher pressure than before [5]. This is achieved through a unique construction of the microscope that includes a differential pumped chamber, separating the tube, where the vacuum is from the specimen chamber where there can be a pressure up to 2 000 Pa [6, 7]. The microscope is equipped with a combined signal

electron detection system that allows recording the sample's image in different contrast modes [8]. Monocrystalline backscattered electron detector incorporating a YAG (Yttrium Aluminum Garnet) of a new type can change the contrast of the image by changing the voltage on the electrodes. The microscope includes a sample cooling device giving up to −30 °C and water vapor permeation and regulation equipment in a specimen chamber working in any pressure range [9]. The limitation of a soft tissue destruction during the pumping process is achieved by the developed method of a cyclic flooding the sample using a water injection built into the specimen chamber.

3. Critical Flow

The gas flow in apertures has specific physical characteristics for given pressure ratios called critical flow. The characteristic phenomenon, which also occurs in our case, is a fast flow through the small aperture which separates significantly different pressures in chambers [10]. The one-dimensional flow of ideal gas gives us the basic idea.

The higher the pressure difference between both sides of the aperture is, the higher the velocity of the flow within the aperture. However, this relation applies only until the moment when the flow through the aperture reaches the velocity of 1 Mach. Then the flow reaches the critical flow, meaning it cannot reach a higher velocity within the aperture than the sound velocity, even when the pressure difference in between the chambers is increasing more. This also means the aperture cannot let pass more gas per time unit through itself than the amount which passes the moment when the gas flows through the aperture at the velocity of 1 Mach, therefore a pressure drop occurs behind the aperture. To determine the mass flow rate of the gas through the nozzle, we use the continuity equation applied in the output cross section of the nozzle. In the modified computational relationship, the mass flow rate through the nozzle depends on the pressure and the density of a gas in the specimen chamber and on the ratio of the pressure on the output of the nozzle and the pressure in the specimen chamber. When the critical state of the flow happens in the output cross section, the critical and its maximum mass flow rate occurs. Other diminution of the pressure of the surroundings could not increase this flow rate – the additional expansion behind the nozzle happens. These realities determine pressure ratios. The ratio of the pressure behind the nozzle p_a and the pressure in the specimen chamber in front of the nozzle p_o:

$$\varepsilon_a = \frac{p_a}{p_o}. \tag{1}$$

The ratio of the critical pressure p_{cr} and the pressure in the specimen chamber in front of the nozzle p_o:

$$\varepsilon_{cr} = \frac{p_{cr}}{p_o}. \tag{2}$$

The subsonic flow of the gas through the nozzle does exist in the range of the pressure ratios $1.0 > \varepsilon_a > \varepsilon_{cr} = 0.5283$ for $\kappa = 1.4$. Up to values of pressure ratios $\varepsilon_a < \varepsilon_{cr}$, the critical mass flow rate of the gas remains constant.

Subcritical flow is for:

$$\varepsilon_a \geq \varepsilon_{cr}. \tag{3}$$

The critical pressure ratio:

$$\varepsilon_{cr} = \frac{p_{cr}}{p_o} = \left(\frac{2}{\kappa+1} \right)^{\frac{1}{\kappa-1}}. \tag{4}$$

In Fig. 2 there are Schlieren pictures, where shades correspond to the gradient of the air refraction index and thus its density. Behind the aperture, there is the area of supersonic flow with a lower pressure forms. The area of transition between lower and higher pressure areas is the point where the flow velocity drops below the speed of sound in a form of shock wave. It is a very thin area of increased density of gas. There are different forms of a shockwave according to the pressure difference, the direction of the flow and other effects.

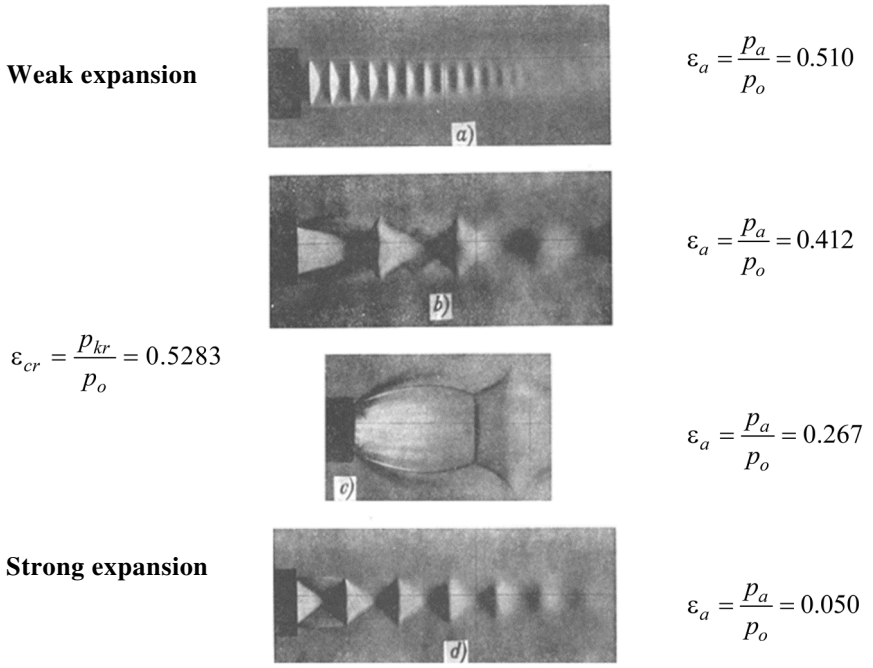

Fig. 2 Critical flow [11]

In Fig. 2 is shown the flow of the real gas behind the output cross section, when due to other expansion rises the area of supersonic flow, which is slowed down in shock-waves. The pictures of flowing flow from the symmetric tapering nozzle are shown in Fig. 2. All developmental stages of the flow structure are well visible, as in case of:

- Weak expansion very close to the suggested regime
- Stronger expansion
- Formation of the shock wave
- Strong expansion and the existence of the shock waves

4. Results

Boundary conditions of the numerical solution are shown in Fig. 3. The gas flow analysis was realized as a simulation of pumping of the differentially pumped chamber. The analysis was solved using the mechanism of continuum method by the Ansys Fluent system [12], which uses the finite volume method [13]. Because of the critical flow which occurs in the examined area, the Density Based Coupled Calculation Scheme with the second upwind discretization with the Advection Upstream Splitting Method (AUSM) was used in the calculation [14, 15].

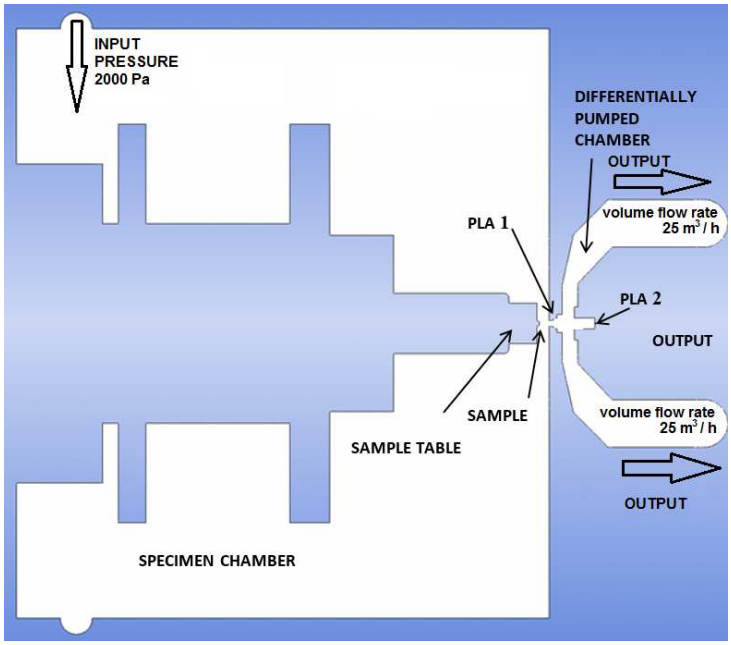

Fig. 3 Boundary conditions

Courses of the gas pressure and velocity in the primary beam path have been examined (Fig. 4) to evaluate the influence of critical flow. Results of the numerical simulation shown in Figs. 5 and 6 prove that with the pressure values above 500 Pa in the specimen chamber, the critical flow in the aperture PLA 1 rises.

The simulation of the flow by the Ansys Fluent system with given dimensions and the shape of the differentially pumped chamber gives us results connected to the critical flow at pressures above the 200 Pa in the specimen chamber. The result of the solution is also determination of the pressure decrease behind the aperture PLA 1.

The result is that with every increase in the pressure ratio between the specimen chamber and the differentially pumped chamber, the pressure drop behind the aperture PLA 1 in the area with supersonic flow increases as well. As shown in Fig. 6, for specified boundary conditions of the solution at operating pressure within the specimen chamber of 2 000 Pa, the pressure within the differentially pumped chamber drops to 250 Pa and the pressure ratio is 0.125, i.e. there is an area of strong expansion behind the PLA 1.

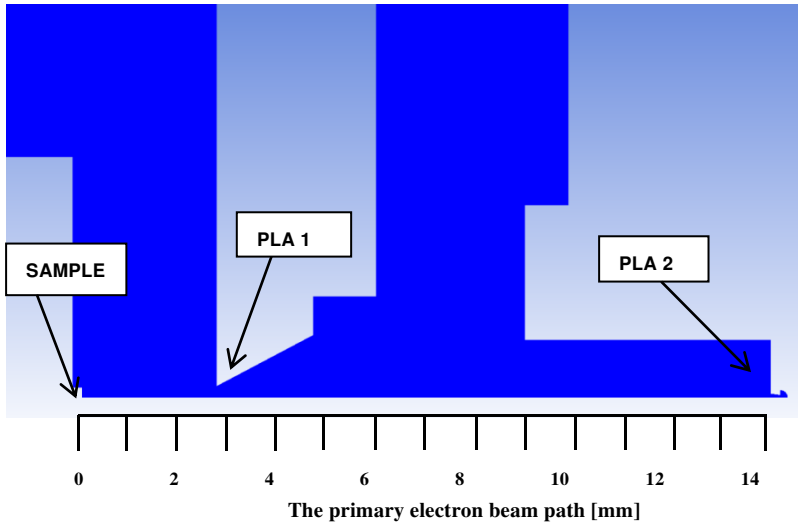

Fig. 4 Scheme of the primary beam path

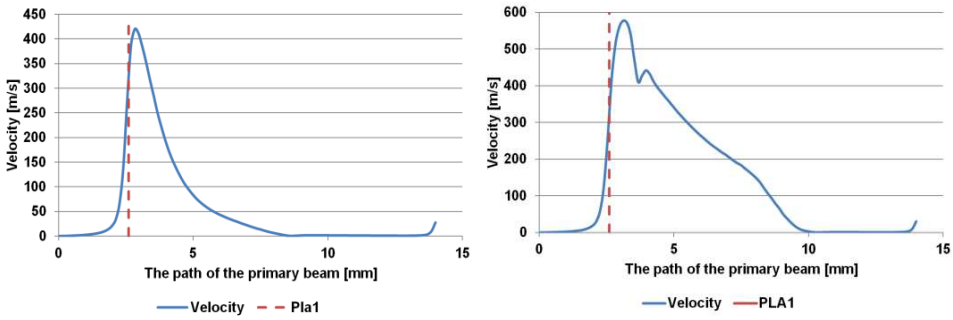

Fig. 5 Course of gas velocity on primary beam path for 500 Pa variant (left) and 2 000 Pa variant (right)

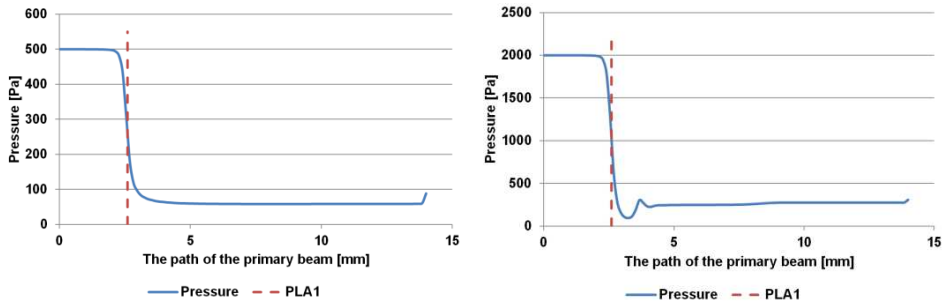

Fig. 6 Courses of gas pressure on primary beam path for cases of 500 Pa variant (left) and 2 000 Pa variant (right)

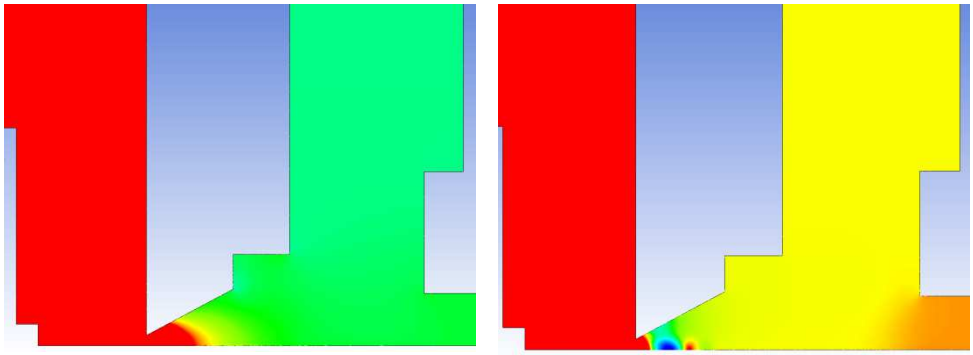

Fig. 7 Color image of the pressure distribution for cases of 500 Pa (left) and 2 000 Pa (right) with shockwave structures

Fig. 7 shows the pressure distribution for two cases of pressure in specimen chamber 500 Pa and 2 000 Pa. Further on, the shockwave is not shaped into a thin zone but into a cloud-like area with an increased pressure. The reason for that is the low ambient pressure behind the aperture. The supersonic flow is always slowed down the area of subsonic flow in shockwaves. Because of the average pressure decrease on the primary electron beam path, the effect mentioned above is applicable when constructing the differentially pumped chamber.

For the given example, it is possible to verify critical quantities according to principles and relationships for the one-dimensional flow:

The critical pressure comes from:

$$p_{cr} = 0.528\, p_0 \,. \tag{5}$$

In the case of 2 000 Pa in the specimen chamber, the critical pressure is: $p_{cr} = 1\,056$ Pa, which respond to the value shown in the graphics in Fig. 6 right.

In the case of 500 Pa in the specimen chamber, the critical pressure is: $p_{cr} = 264$ Pa, which also respond to the value shown in the graphics in Fig. 6 left.

It is also appropriate to express the value of the critical velocity. In fact, that the critical velocity is not the function of the pressure but the temperature, it is possible to use the following equation:

$$V_{cr} = \sqrt{\frac{2\kappa}{\kappa+1} RT_0} \tag{6}$$

$$V_{cr} = 313.2 \text{ ms}^{-1}$$

The result responds to the values shown in graphics in Fig. 5.

From the comparison of the critical pressure values and of the critical velocity follows, that the one-dimensional flow provides the same results with the modeling by the CFD system.

5. Knudsen Number

Since it is about the calculations in the area of low pressures is necessary to evaluate the value of the Knudsen number, for the evaluation of the flow character in the solving area, whether it is continuous area where Stock-Navier equations apply.

The Knudsen number should be checked [16] by Eq. (7).

$$Kn = \frac{\lambda}{L}. \tag{7}$$

where λ is the mean free path of gas molecules [m] and L is the characteristic dimension [m].

$$\lambda = \frac{kT}{\sqrt{2}\pi\delta^2 p}. \tag{8}$$

where k is the Boltzmann constant, T is the absolute temperature [K], δ is the gas molecule diameter [m], p is the pressure [Pa]. According to the value of the Knudsen number, it is possible to evaluate the character of the flow. It applies:

$Kn < 0.1$	Continual (viscous) flow
$0.1 < Kn < 0.5$	Transitional flow
$Kn > 0.5$	Molecular flow

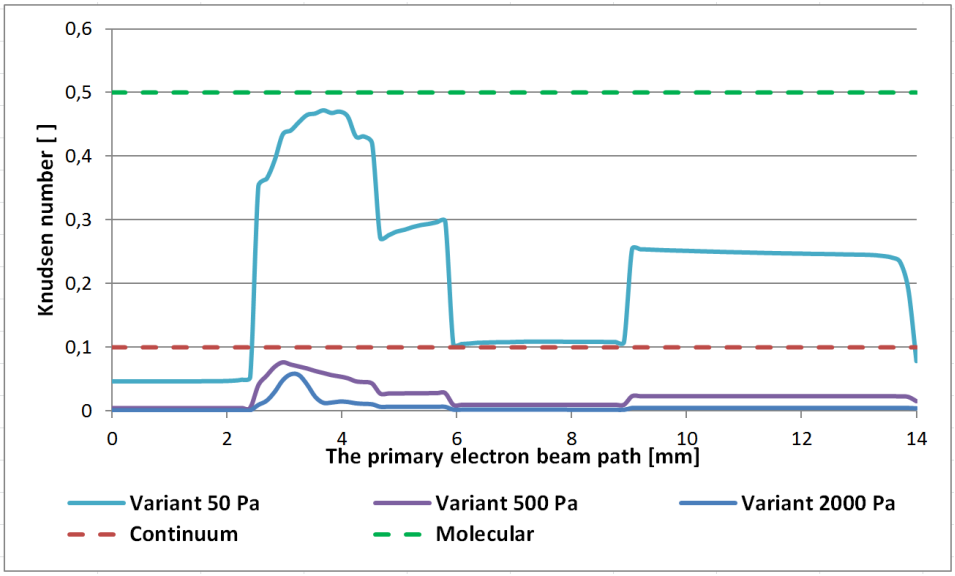

Fig. 8 Knudsen number for chosen variants

The course of the Knudsen number along the primary electron beam path (see Fig. 4) is shown in Fig. 8. The results show that up to a value of the pressure of 200 Pa in the specimen chamber, the flow in the calculating area has the character of a mechanism of continuum. If the specimen chamber pressure is less than 200 Pa, the value of the Knudsen number is in the transition flow range in some places. This case is shown in Fig. 8 in the 50 Pa variant. It is true that even in this variant of 50 Pa in the specimen chamber the value of the Knudsen number is not in the molecular flow, but only in the transitional flow area, but for this reason the results will be checked on the experimental model.

The course of the Knudsen number determines the possibilities of use of CFD simulations for solving of the gas flowing at low pressures. The results show that for a given example of a differential chamber construction, in a variation where the spec-

imen chamber has a pressure lower than 200 Pa, flow occurs in the character of the transient flow in some areas. CFD does not provide corresponding results here.

For this reason, the experimental measuring will be done on the experimental chambers made for this purpose, to verify current results. On these experimental chambers will be mapped the character of the flow also for variants below 200 Pa in the specimen chamber, where transitional flow occurs. These results will be compared with the results obtained from CFD for this area, where CFD might have problem because of the value of the Knudsen number above 0.1.

6. Conclusions

Due to the wide possibilities, which the electron microscopy offers, is its using in the military totally necessarily to maintain the defense on the high level. One of the inventions that would not be possible without the electron microscopy is the development of the composite plastic, which is equal with its strength to the steel, but is much lighter and transparent. This plastic was created by scientist at the University in Michigan, by mimicking the molecular structure which was found in seashells. The invention should lead, for example, to designing lighter and stronger armors for soldiers or police and of course also for their vehicles. The effort is to make this material absorb the energy from the projectile. US Department of Defense is interested in this field in the development of more effective armor for unmanned aircrafts of the air forces, but also for the vehicles and other fields of armed forces.

For the purposes of the army for using in terrain was also directly developed electron microscope Mini SEM.

Acknowledgement

We would like to thank to Ing. et. Ing. Vilém Neděla Ph.D. from Institute of Scientific Instruments of the Czech Academy of Sciences in Brno for consultations in given issues. Publication was supported by the internal grant FEKT-S-14-2293 (Materials and technology for electrical engineering II).

References

[1] NEDĚLA, V. Controlled Dehydration of a Biological Sample using an Alternative form of Environmental SEM. *Journal of Microscopy, 2010*, vol. 237, no. 1, p. 7-11. ISSN 0022-2720.

[2] DANILATOS, G.D. Velocity and Ejector-jet Assisted Differential Pumping: Novel Design Stages for Environmental SEM. *Micron*, 2012, vol. 43, no. 5, p. 600-611. DOI 10.1016/j.micron.2011.10.023.

[3] NEDĚLA, V., KONVALINA, I., LENCOVÁ, B. and ZLÁMAL, J. Comparison of Calculated, Simulated and Measured Signal Amplification in Variable Pressure SEM. *Nuclear Instruments & Methods in Physics Research Section A*, 2011, vol. 645, no. 1, p. 79-83. DOI 10.1016/j.nima.2010.12.200.

[4] ORAL, M., NEDĚLA, V. and DANILATOS, G.D. Dynamic Correction of Higher-Order Deflection Aberrations in the Environmental SEM. *Microscopy and Microanalysis*, 2015, vol. 21, no. 4, p. 194-199. DOI 10.1017/S1431927615013367.

[5] NEDĚLA, V., HŘIB, J., HAVEL, L., HUDEC and J., RUNŠTUK, J. Imaging of Norway Sruce Early Somatic Embryos with the ESEM, Cryo-SEM and Laser Scanning Microscope. *Micron,* 2016, vol. 84, p. 67-71. ISSN 0968-4328.

[6] NEDĚLA, V., HŘIB, J. and VOOKOVÁ, B. Imaging of Early Conifer Embryogenic Tissues with the Environmental Scanning Electron Microscope. *Biologia Plantarum*, 2012, vol. 56, no. 3, p. 595-598. ISSN 0006-3134.

[7] TIHLAŘÍKOVÁ, E., NEDĚLA, V. and SHIOJIRI, M. In Situ Study of Live Specimens in an Environmental Scanning Electron Microscope. *Microscopy and Microanalysis*, 2013, vol. 19, no. 4, p. 914-918.
DOI 10.1017/S1431927613000603.

[8] JIRÁK, J., NEDĚLA, V., ČERNOCH, P., ČUDEK, P. and RUNŠTUK, J. Scintillation SE Detector for Variable Pressure Scanning Electron Microscopes. *Journal of Microscopy, 2010*, vol. 239, no. 3, p. 233-238. ISSN 0022-2720.

[9] NEDĚLA, V., KONVALINA, I., ORAL, M. and HUDEC, J., The Simulation of Energy Distribution of Electrons Detected by Segmental Ionization Detector in High Pressure Conditions of ESEM. *Microscopy and Microanalysis*, 2015, vol. 21, no. 4, p. 264-269. DOI 10.1017/S1431927615013483.

[10] VYROUBAL, P., MAXA, J., NEDĚLA, V., JIRÁK and J., HLADKÁ, K. Apertures with Laval Nozzle and Circular Orifice in Secondary Electron Detector for Environmental Scanning Electron Microscope. *Advances in Military Technology,* 2013, vol. 8, no. 1, p. 59-69. ISSN 1802-2308.

[11] DEJČ, M.J. *Technical Dynamics of Gases* [in Czech]. Prague: SNTL, 1967, 660 p.

[12] ANSYS Inc. *ANSYS Web Help* – PDF Documentation for Release 15.0 [online]. [cited 2016-05-08]. Available from: <http://148.204.81.206/Ansys/readme.html>.

[13] MAXA, J., BÍLEK, M., HLAVATÁ, P.; VYROUBAL, P. and LEPLTOVÁ, K. Comparisons Using Methods of Continuum Mechanics and Monte Carlo at Differentially Pumped Chamber. *Advances in Military Technology*, 2016, vol. 11, no. 2, p. 143-150. DOI 10.3849/aimt.01120.

[14] MAXA, J. and NEDĚLA, V. The Impact of Critical Flow on the Primary Electron Beam Passage through Differentially Pumped Chamber. *Advances in Military Technology*, 2011, vol. 6, no. 1, p. 39-46. ISSN 1802-2308.

[15] MAXA, J., NEDĚLA, V., JIRÁK, J., VYROUBAL, P. and HLADKÁ, K. Analysis of Gas Flow in a Secondary Electron Scintillation Detector for ESEM with a New System of Pressure Limiting Apertures. *Advances in Military Technology*, 2012, vol. 7, no. 2, p. 39-44. ISSN 1802-2308.

[16] URUBA, V. *Turbulence Handbook for Experimental Fluid Mechanics Professionals.* Skovlunde: Dantec Dynamic, 2012, 148 p.